J. Indian Chem. Soc.,
Vol. 97, No. 11a, November 2020, pp. 2144-2154

Manganese(II), cobalt(II), nickel(II), copper(II) and zinc(II) complexes of sulfathiazole functionalised Schiff base: Synthesis, characterization, redox behavior, antioxidant and antimicrobial activities

I. Rama* and R. Selvameena

P.G. and Research Department of Chemistry, Seethalakshmi Ramaswami College (Autonomous),

Affiliated to Bharathidasan University, Tiruchirappalli-620 002, Tamil Nadu, India

E-mail: rama14jai@yahoo.co.in

Manuscript received online 01 October 2020, revised and accepted 27 November 2020

Metal chelates of Mn(II), Co(II), Ni(II), Cu(II) and Zn(II) acetates with Schiff base ligand obtained from sulfathiazole and 5–nitro salicylaldehyde (HL) have been synthesized. The structural traits of the ligand and its complexes have been construed by microanalytical data, electrical conductance, FT-IR, ^{1}H and ^{13}C NMR, UV-Visible spectra, magnetic moment studies, thermal analysis, EI-mass spectra and powder XRD studies. The Schiff base is coordinated to metal through two donor atoms and is azomethine nitrogen and deprotonated phenolic oxygen atoms. Thermogravimetric studies of metal complexes show multistep decay and EI-mass spectra of ligand and complexes support the proposed structure. The complexes are envisaged to have the general formula $[M(L)_2(H_2O)_2]$, where M = Mn(II)/Co(II)/Ni(II)/Cu(II)/Zn(II). Octahedral environs have been put forward for all the metal chelates. To examine the reduction and oxidation property of the synthesized complexes the cyclic voltammetric studies have been executed. The antioxidant and antimicrobial effect of them were also explored. The antioxidant property of the ligand is significant, which on complexation with metals show a decrease in the activity against ABTS assay.

Keywords: Sulfathiazole, ligand, spectral characterization, complexes, antioxidant activity, antimicrobial activity.

Introduction

For the past few decades, Schiff bases have been a center of attention and attraction for chemists and biologists because of their wide structural and pharmacological relevance[1]. The scope of diverse kinds of amines and carbonyl compounds facilitated the preparation of Schiff bases with different structural facets. The bonding capability of the ligand depends on the character of atoms that act as bonding sites, their steric effect and electronegative character. Because of the lone pair of electrons on the nitrogen atom, electron donor nature of the double bond, less electronegativity over nitrogen and good donor property of the nitrogen of azomethine group (>C=N) makes the Schiff base more active. The coordination complex thus formed is highly stable when the resultant ring becomes five or six membered. Hence the stability is enhanced by the existence of azomethine group with replaceable hydrogen atom near to >C=N. To avoid the rapid decomposition or polymerization, an aryl group should be tied to the nitrogen or to the carbon of the -C=N- double bond. Schiff bases have been found to be biologically active and show excellent biological properties[2] such as anti-oxidant, antiviral, antibacterial, antifungal and many other properties.

The sulfonamides and their N-derivatives are currently prevailing functional groups for their biological applications among the different categories of organic-inorganic chemicals investigated so far. A sequence of new derivatives of sulfamethoxazole has been explored for its antimicrobial activity[3]. The docking studies on the sulfamethoxazole drug candidate over the receptors DHPS and DNA were reported[4]. The cytotoxic studies on sulfamethoxazole derivative and its copper complex exhibit significant *in vitro* anticancer activity[5,6]. Schiff bases of sulfathiazole shows very fine antibacterial activity and has good docking score with DHPS protein[7]. Sulfathiazole is one of the most used sulfa drug clinically. A look for the literature disclosed that no work has been done on transition metal chelates of the azo-imine derivative obtained from sulfathiazole and 5-nitro salicylaldehyde. The

synthesis of ligand is performed by treating sulfathiazole and 5-nitro salicylaldehyde. The complexes of Mn(II), Co(II), Ni(II), Cu(II), and Zn(II) with this ligand were prepared and characterized using different physico-chemical methods.

Experimental

All reagents and chemicals purchased from High media chemicals were of AR grade and used as such. The composition of the complexes was arrived at by estimating the metal and anions besides the microanalysis (CHNS) of complexes. The metals were estimated by the ICP-AES method. The physical constant value (melting point) of all the compounds was examined by inserting the sample in glass capillary tubes and heated in a digital melting point apparatus containing silicon bath attached with stirrer and are uncorrected. The complexes dissolved in DMF (10^{-3} *M*) was used to detect the molar conductance at 28±2°C using a Elico conductivity bridge. The cell constant of the conductivity cell used was 0.983 cm^{-1}. Infrared spectral measurements were made for the ligand and its complexes in KBr pellet using infrared spectrometer in the region 4000–400 cm^{-1}. The proton and ^{13}C NMR of ligand were recorded using DMSO-d_6 as solvent.

The absorption spectra of the ligand and its complexes were obtained from UV-Visible region with working range of 200 nm–1100 nm. The magnetic properties of all the complexes were followed through the use of Gouy balance at room temperature (28±2°C). The EPR studies were performed at both liquid nitrogen temperature and room temperature.The thermal behavior was examined using Perkin-Elmer, Diamond TG/DTA model. Mass spectra were recorded and analysed in EI mode. The powder XRD studies were accomplished using Bruker AXS D8 Advance diffractometer. Cyclic voltammetry studies were achieved using a three electrode cell configuration. The instruments utilised include an EG and GPAR 273 potentiostat/Galvanost at and Pentium IV computer with EG and GM270 software to do the experiments and to obtain the data.

Experimental procedure for antioxidant activity:

The antioxidant property of the synthesized Schiff base and its chelates has been examined using DPPH and ABTS free radical assay[8,9]. The radical scavenging activity was represented as the percentage inhibition and was computed using the formula:

$$\% \text{ of Inhibition} = [(A_0 - A_1)/A_0] \times 100$$

where A_0 is the absorbance of the control and A_1 is the absorbance of the compound.

Synthesis of ligand HL (NSST):

A stirred DMF-ethanolic solution of sulfathiazole (0.765 g, 0.3 mmol) and ethanolic solution of 5-nitro salicylaldehyde (0.501 g, 0.3 mmol) were mixed and was heated in hot plate and stirred for 4 h. The yellowish orange Schiff base obtained was washed with ethanol and dried, recrystallised and checked for purity by TLC.

Synthesis of metal complexes:

Ethanolic solution of corresponding metal acetate (0.1 mmol) was treated with a ligand (0.2 mmol) dissolved in DMF-ethanol mixture. They were stirred and heated for 10 h, and the solid product was collected on through filtration and washed with petroleum ether and recrystallised.

Results and discussion

The reaction of one equivalent of sulfathiazole with equal quantity of 5-nitro salicylaldehyde leads to the formation of ligand HL (Scheme 1). Direct interaction of two equivalent aliquots of Schiff base with one equivalent aliquot of metal species such as manganese, cobalt, nickel, copper and zinc acetate yield the corresponding metal derivatives in 1:2 (M:L) ratio.

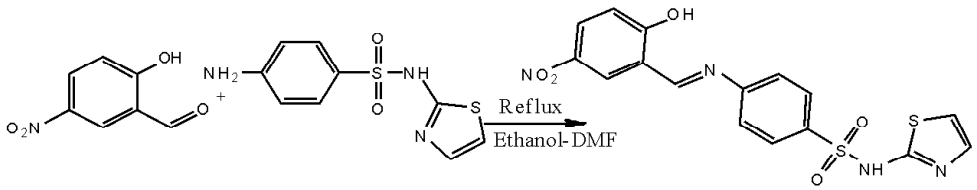

(*E*)-4-((2-hydroxy-5-nitrobenzylidene)amino)-*N*-(thiazol-2-yl)benzenesulfonamide(HL)

Scheme 1

Characterization of synthesized compounds

Analytical data:

The formation of the ligand has been ascertained by microanalytical data, FT-IR, ^{1}H, ^{13}C NMR spectroscopy, UV-Visible and EI-mass spectrometry. The ligand melts at high temperature and is very sharp. The TLC pure ligand is soluble in high polar solvents like dimethyl formamide, dimethyl sulfoxide and dioxan and insoluble in most of the organic solvents. The synthesized metal complexes (**1-5**) are very stable and non-hygroscopic in nature. The complexes have been subjected to metal estimation, elemental analysis, electrical conductance, FT-IR, UV-Visible, magnetic moment, EPR, thermal, mass spectral and powder XRD studies to arrive at the probable structures of the complexes. The microanalytical data are agreeable to the suggested structure of the ligand and complexes.

Molar conductance:

The conductance value of all the compounds is within the scale of 17.91–19.79 W^{-1} cm^2 mol^{-1}. The entire complexes exhibit low conductance values less than 35 Ω^{-1} cm^2 mol^{-1}, which are indicative of the non-electrolytic nature of the complexes[10].

Structure establishment through spectral data:

Analysis of the vibrational spectral data of the complexes with that of ligand guides to comprehend the donor sites of the ligand molecule. In the infrared spectrum of the ligand a medium intensity band appears at 3241 cm^{-1} caused by phenolic ν(-OH)[11]. This band vanishes after chelation with the metal ion, which implies the removal of proton from the -OH group of the ligand before coordination via the oxygen atom[12]. A strong band at 1622 cm^{-1} attributable to the azomethine group[13] of the ligand experience a major shift by 12–34 cm^{-1} after bonded to metal ion, indicating coordination of the nitrogen from azomethine group to metal species[14]. A high intense dip at 1481 cm^{-1} in the ligand may be consigned to the phenolic C-O stretching frequency. After chelation, major shifts of C-O stretching vibrations are observed by 11–16 cm^{-1}. This shift implies that there is a bond formation via the phenolic oxygen atom[15]. New bands arises at low frequency region after complexation and are located in between the range of 569–572 cm^{-1} and 402–486 cm^{-1} which are owing to ν(M-O)[16] and ν(M-N)[17]. The occurrence of a broad band in the range of 3417–3477 cm^{-1} evinces the presence of coordinated water in all the complexes[18].

The ^{1}H NMR spectrum of the ligand, authenticates the formation of Schiff base by the existence of singlet at 9.123 ppm corresponding to azomethine[19] proton (-CH=N-). In the spectrum the phenolic proton signal observed for HL is at 12.422 ppm. All the other protons have been found in the expected region[20]. The ^{13}C NMR spectrum of the ligand HL, exhibits signals because of the carbon atoms attached to the azomethine group and phenolic group in ligand appears[21] at 165.84 ppm and 162.57 ppm respectively.

The electronic spectrum of HL exhibits two bands at 276 nm (36,232 cm^{-1}) and 293 nm (34,130 cm^{-1}) assignable to $\pi \rightarrow \pi^*$ transition[22]. The electronic absorption peaks manifested in the regions 348 nm (28,736 cm^{-1}) and 532 nm (18,789 cm^{-1}) are assigned to $^{6}A_{1g} \rightarrow {}^{4}A_{1g}(^{4}G)$ and d-d transitions respectively, for the complex **1** (Fig. 1a) strongly ratify six coordinated octahedral geometry[23]. The magnetic moment values for complex **1** is 5.93 B.M. at room temperature, which is very nearer to high spin six coordinated octahedral configuration[24]. The μ_{eff} of complex **2** has been observed to be 4.79 B.M. as anticipated for high spin octahedral Co(II) complexes[25]. The spectrum of complex **2** (Fig. 1b) shows two intense maxima at 428 nm (23,364 cm^{-1}) and 594 nm (16,835 cm^{-1}). These bands are attributable to the $^{4}T_{1g}(F) \rightarrow {}^{4}T_{1g}(P)$ (ν_3) and $^{4}T_{1g}(F) \rightarrow {}^{4}A_{2g}(F)$ (ν_2) transitions[26]. The λ_{max} value of complex **3** exhibits absorption bands at

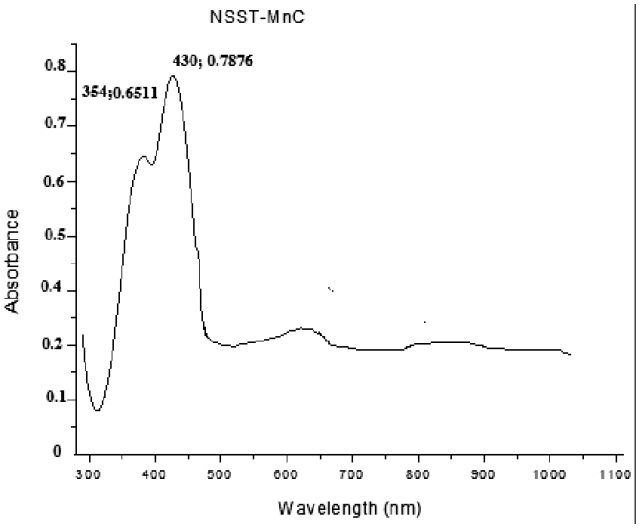

Fig. 1a. Electronic spectrum of complex **1**.

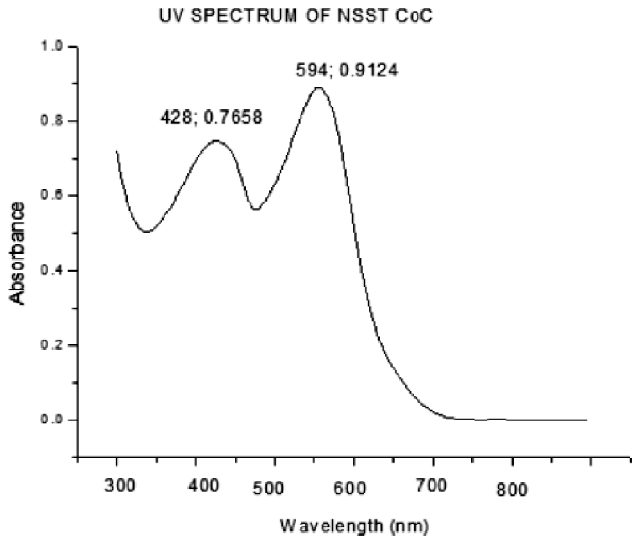

Fig. 1b. Electronic spectrum of complex **2**.

550 nm (18,182 cm^{-1}) and 920 nm (10,870 cm^{-1}) and these intense bands observed are normally predictable for an octahedral configuration[22] and may be caused by the transitions $^3A_{2g}$ $(F)\rightarrow{}^3T_{1g}$ (P) (ν_3) and $^3A_{2g}$ $(F)\rightarrow{}^3T_{1g}$ (F) (ν_2) respectively. The value of magnetic susceptibility (3.04 B.M.) shows the existence of two unpaired electrons for Ni(II) ion implying an octahedral arrangement[27] for complex **3**. The μ_{eff} value of complexes **4** (1.66 B.M.) is supporting octahedral environment for copper complex[28]. The UV-Visible spectrum of complex **4** shows one band at 660 nm (15,152 cm^{-1}) and another band at 330 nm (30,303 cm^{-1}). The first band is assigned to the transition $^2E_{1g}\rightarrow{}^2T_{1g}$ and second band corresponds to metal to ligand charge transfer[29]. A high energy band at 340 nm (29,422 cm^{-1}) for the complex **5** in the UV spectrum is due to charge transfer transition. The diamagnetic property of the zinc complex is revealed by the magnetic susceptibility measurements.

The molecular ion peak of the ligand HL shows *m/z* value 404.40, which is nearly equal to the molecular weight of the formed Schiff base. The ligand shows one important peak with 100% abundance with *m/z* = 180 attributes to the fragmented molecular ion after elimination of thiazole and nitro salicylidene moieties with molecular formula $(C_7H_7N_2O_2S)^+$. The mass spectra of complexes **1**, **3** and **5** display the molecular ion peaks that support the molecular mass of the proposed structures.

Manganese complex is subjected to X-band EPR analysis at room temperature, shows *g* value of 2.037 at room temperature supports the octahedral geometry[30]. The EPR spectrum of complex **4** at liquid nitrogen temperature unveils four peaks, which are well resolved at low field region. From the peak positions *g*-values evaluated are $g_{||}$ = 2.27 and $g_{\perp}$ = 2.12. The exploration of spectrum gives $g_{||} > g_{\perp} >$ 2.0023, indicate that unpaired electron is well situated in $d_{x^2-y^2}$ orbital of tetragonally elongated octahedral geometry. The g_{av} and $g_{||}/A_{||}$ has been calculated to be 2.17 and 151 respectively[31].

The coupling constant (λ) has been evaluated by the formulae $g_{av} = 1/3[g_{||} + g_{\perp}]$ and $g_{av} = 2(1\text{-}2\lambda/10Dq)$ and is found to be –436 cm^{-1}. The λ obtained is a smaller value when compared with the free Cu(II) ion (–832 cm^{-1}) which illustrates covalent nature of metal-ligand bond in the complex. This observation is confirming the octahedral environ around central metal ion (copper). The axial factor *G* is calculated by using relation $(g_{||}\text{-}2/g_{\perp}\text{-}2)$ and is 2.25. The *G* value which is less than four corroborates the subsistence of some exchange interactions between the copper centers. The $g_{||} <$ 2.3 indicates a considerable extent of covalency in Cu-L bonding. From the EPR spectral data and d-d transition band values the bonding parameter α^2 has been delineated. The parameter is a quantifier of covalent nature of in-plane σ bond and is measured using the expression $\alpha^2 = -(A_{||}/0.036) + (g_{||} - 2.0027) + (3/7)(g_{\perp} - 2.0027) + 0.04$. The values of α^2 for the complex is 0.54 corborating that the in-plane σ bonds are appreciably covalent[32].

	g tensors			Bonding parameters			
Complex	$g_{||}$	$g_{\perp}$	g_{av}	$g_{||}/A_{||}$	λ	α^2	*G*
$[Cu(L)_2(H_2O)_2]$	2.27	2.12	2.17	151	–436	0.54	2.25

Thermal analysis:

Thermal degradation of complexes (Table 1) may be useful for substantiating predicted structure through weight loss during decomposition or oxidation. From the TGA curve of the complex **4**, it is observed that there is approximately 3.94% weight loss is observed (calculated 3.97%) in the range of 127–162°C. This is the evidence for the complex contains two coordinated water molecules in the complex. A huge

Table 1. TGA/DTA data of metal(II) chelates

Metal complexes	Stage	Temperature (°C)		Loss in weight (%)		Reason for weight loss
		TGA	DTA	Observed	Calcd.	
$[Cu(L)_2(H_2O)_2]$	I	127–162	133.46	3.94	3.97	Two molecules of coordinated water
	II	170–320	254.44	87.34	88.07	Two molecules of ligand moiety
	III	310–400	353.91	10.32	9.30	Metal oxide
$[Zn(L)_2(H_2O)_2]$	I	130–146	138.21	3.92	3.97	Two molecules of coordinated water
	II	205–467	315.33	86.30	46.7	One molecule of ligand moiety
	III	320–400	346.41	46.71	46.57	One molecule of ligand moiety

weight loss has been found in the second stage and shows mass loss in between the heating range of 170 and 320°C (observed 87.34%, calculated 88.07%) is attributed to the breakdown of two molecules of ligand moieties. In third stage, the thermogram indicates a complete decomposition to the corresponding metal oxide (observed 10.32%; calculated 9.30%). In the TGA thermogram of complex **5** a minimum mass loss in the temperature range of 130–146°C is noticed. The decrease in weight observed is 3.92% (calculated 3.97%) is assigned to decomposition of two coordinated water molecules. A highest and steady weight reduction is observed in between 205 and 467°C is ascribed to the disintegration of two ligand moieties (observed 86.30%; calculated 88.80%). A constant weight is observed above the temperature 480°C, be a sign of the metal constituent in the complex (observed 10.2%; calculated 8.9%).

Powder XRD analysis:

The PXRD studies of complex **4** have been probed by scanning through 5–100° at the λ of 1.5406 Å. The indexing of relative intensity for major peaks (>10%) are executed by using High score plus PXRD software. The unit cell values of complex are refined with parameters a = 19.5678 Å, b = 18.3318 Å, c = 16.5753 Å, and V = 5945.77 Å^3. The complex crystallizes in face centered orthorhombic crystal system with $a \neq b \neq c$; $\alpha = \beta = \gamma = 90°$.

Electrochemical behaviour of metal complexes:

The redox nature of the complexes (**1-5**) has been examined in the potential range of +2.0 V to –2.0 V by dissolving them in DMSO (Table 2). The typical cyclic voltammogram of complex **1** (Fig. 3a) has, on the direct (cathodic) scan, three cathodic waves with a first cathodic wave peak situated at negative cathodic potential and with a second cathodic peak situated at less positive cathodic potential and a third cathodic wave peak situated at more positive potential. On the reverse (anodic) scan there is a shoulder peak, which is the counter peak of the first cathodic peak is obtained with a potential difference of 590 mV suggest a quasi-reversible one electron transfer kinetics[33] with i_{pa}/i_{pc} ratio of 1.190. The second and third cathodic peaks are irreversible in nature. In cobalt complex (**2**) three cathodic peaks were observed with

Table 2. Electrochemical data of metal complexes

Sr. No.	Metal complexes	E_{pa} (V)	E_{pc} (V)	ΔE_p (mV)	i_{pa} (A)	i_{pc} (A)	i_{pa}/i_{pc}
1.	$[Mn(L)_2(H_2O)_2]$	–1.0	–0.41	590	0.499×10^4	0.42×10^4	1.190
		–	0.1	–	–	0.42×10^4	-
		–	0.5	–	–	0.99×10^4	-
2.	$[Co(L)_2(H_2O)_2]$	0.24	0.89	650	0.38×10^4	1.28×10^4	0.297
		–1.20	–0.38	820	0.60×10^4	0.30×10^4	2.00
		–1.90	–	–	0.74×10^4	–	-
3.	$[Ni(L)(H_2O)_2]$	–1.0	0.12	1120	0.16×10^4	0.17×10^4	0.941
4.	$[Cu(L)_2(H_2O)_2]$	–1.4	–0.49	910	0.80×10^4	0.76×10^4	1.06
		–	0.7	–	–	0.72×10^4	-
		–	0.4	–	–	0.65×10^4	-
5.	$[Zn(L)_2(H_2O)_2]$	–1.35	–0.01	1340	$0.57x10^4$	0.60×10^4	0.95

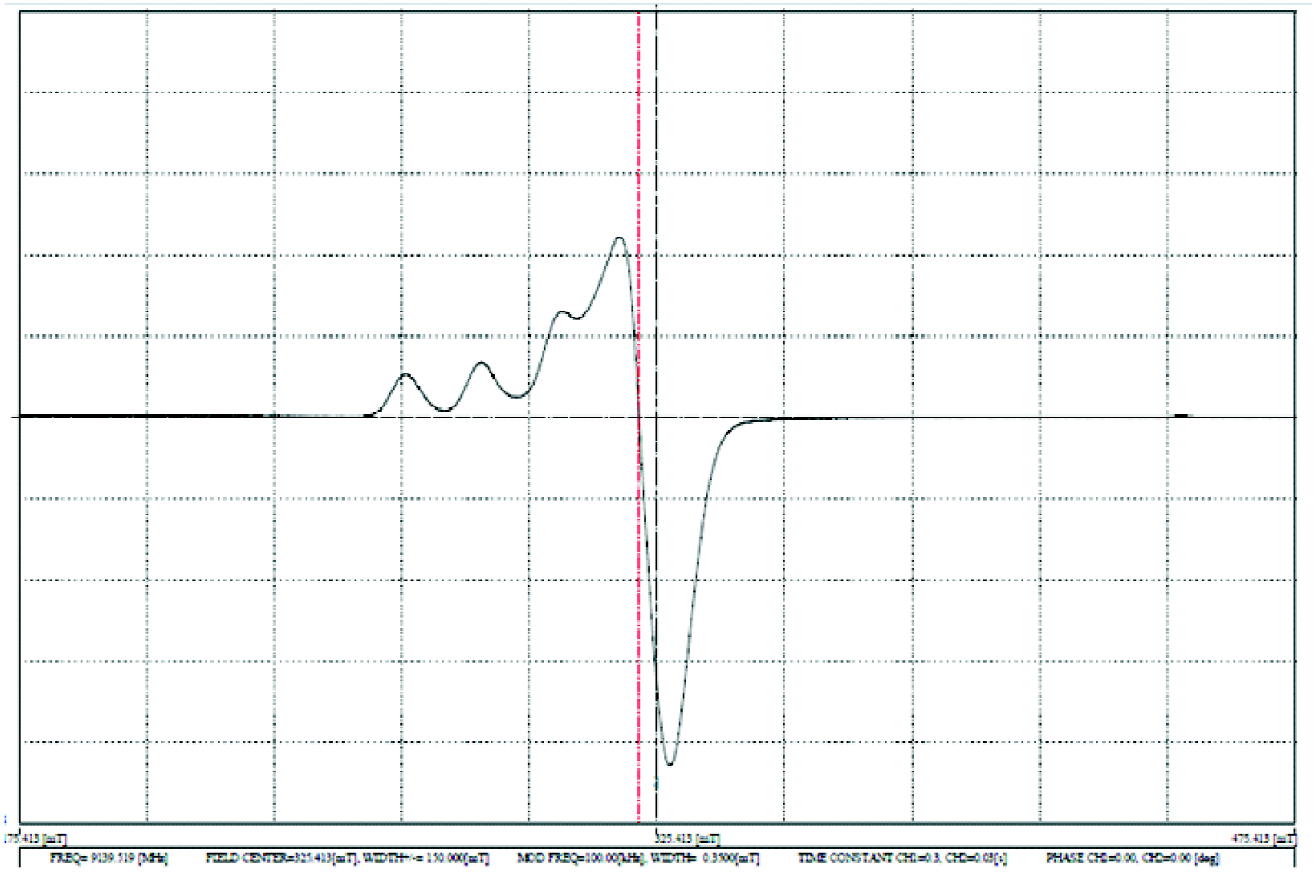

Fig. 2. Electron paramagnetic resonance spectrum of complex **4**.

E_{pa} value of 0.24 V, –1.20 V and –1.90 V. Two anodic peaks were detected at 0.89 V and –0.38 V. The difference between the first cathodic and its relative anodic peak is found to be 650 mV. Similarly the second cathodic peak and its successive anodic peak give a difference of 820 mV with i_{pa}/i_{pc} value of two. Thus the redox behavior of the complex **2** (Fig. 3b) shows quasi-reversible two electron transfer process. The nickel complex (Fig. 3c) shows single cathodic

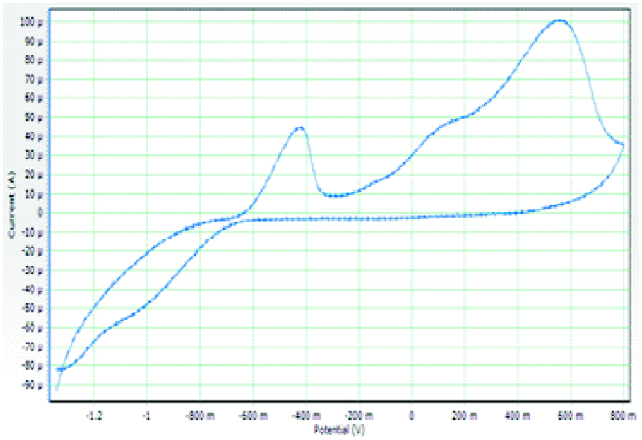

Fig. 3a. Cyclic voltammogram of complex **1**.

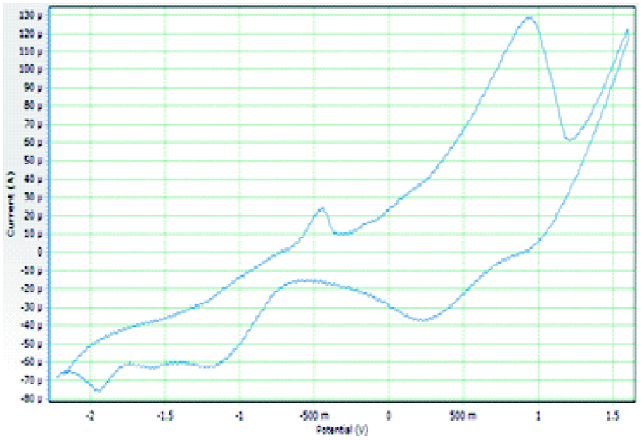

Fig. 3b. Cyclic voltammogram of complex **2**.

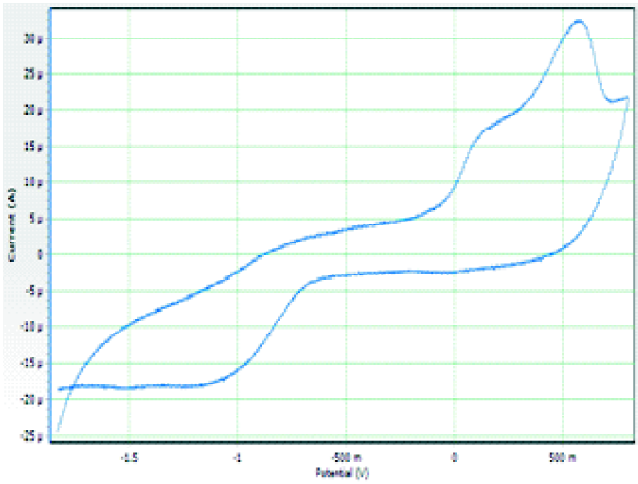

Fig. 3c. Cyclic voltammogram of complex **3**.

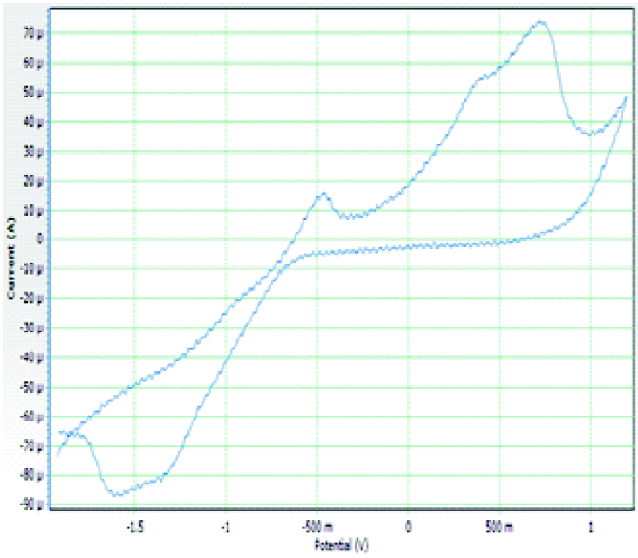

Fig. 3d. Cyclic voltammogram of complex **4**.

and anodic peaks. The relative peak difference is found to be 1120 mV, which clearly infers that the redox couple is not reversible. A single cathodic peak and three anodic peaks are viewed in the voltammogram of copper complex (Fig. 3d). The ΔE_p value is found to be 910 mV, which may be due to irreversible nature of metal centers within the investigated potential range[34]. The i_{pa}/i_{pc} ratio is observed to be 1.06, shows one electron transfer between the metal centers of the redox couple. The complex **5** (Fig. 3e) shows cathodic and anodic peaks with a difference of about 1340 mV with i_{pa}/i_{pc} value of 0.95. The trend is reflected by the unusual

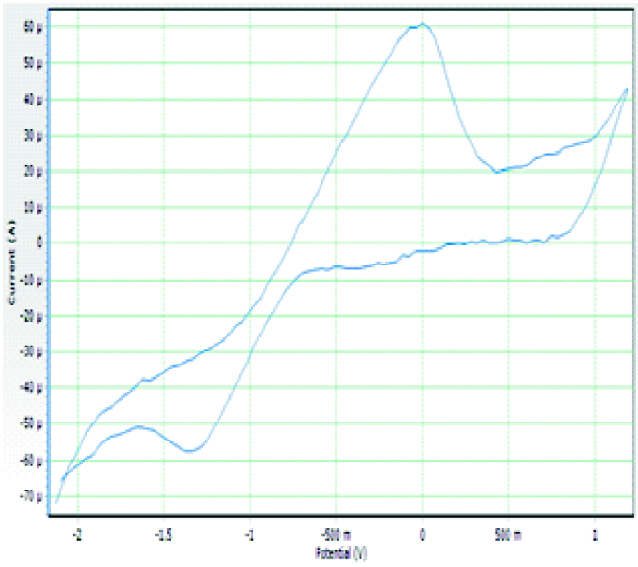

Fig. 3e. Cyclic voltammogram of complex **5**.

values of ΔE_p (1340 mV), not following the reversibility criterion[35]. On comparison of the $\Delta E_p/n$ values of the complexes, they follow the order: Co(II) < Mn(II) < Cu(II) < Ni(II) < Zn(II) confirms the decrease in reversible character of the respective redox couple.

Antimicrobial activity:

The synthesized compounds are subjected to antimicrobial screening towards the bacteria and fungi (Fig. 4a, 4b). The results of activity are presented in the Table 3a and also through graph (Fig. 4c). The ligand HL is observed to have significant biological behavior. After chelation with metals all the complexes are highly active and have very high zone of inhibition value of 21 mm for the complex **5** against *Klebsilla* sp. In most of the complexes the antibacterial activity progressively increases to twice than the ligand. From the data it is proved that the activity of zinc complex is remarkably increased to a greater extent. The ligand HL shows a very weak antifungal activity. The drastic increase in the fungicidal activity of its complexes is noteworthy.

Minimum inhibitory concentration (MIC):

The zinc complex is opted to perform, MIC studies (Table 3b). The MIC is measured using the disc diffusion method (Fig. 4d) at different concentrations (25, 50, 75, 100 μg/ml) by using the same procedure. The complex has pronounced biological activity against the tested microorganism at the

Fig. 4a. Antibacterial activity of HL and its complexes against *Staphylococcus aureus*, *Bacillus subtilis* and *Eschericsia coli.*

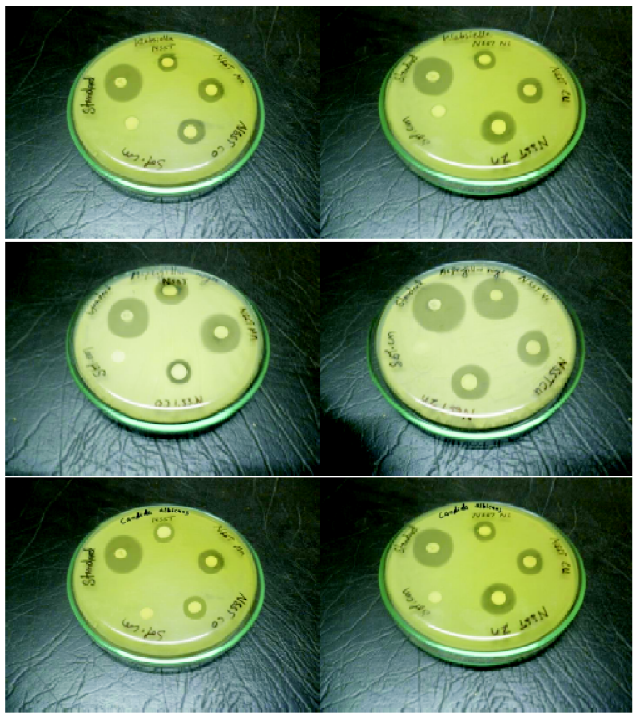

Fig. 4b. Antibacterial activity of HL and its complexes against *Klebsiella* sp. and antifungal activity against *Aspergillus niger* and *Candida albicans.*

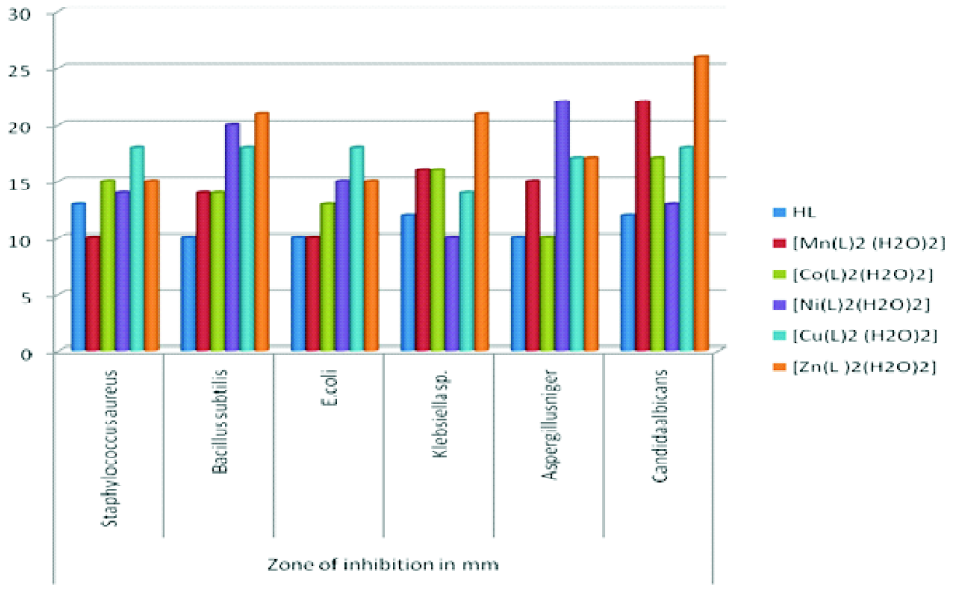

Fig. 4c. Graphical representation of antimicrobial property of HL and its complexes.

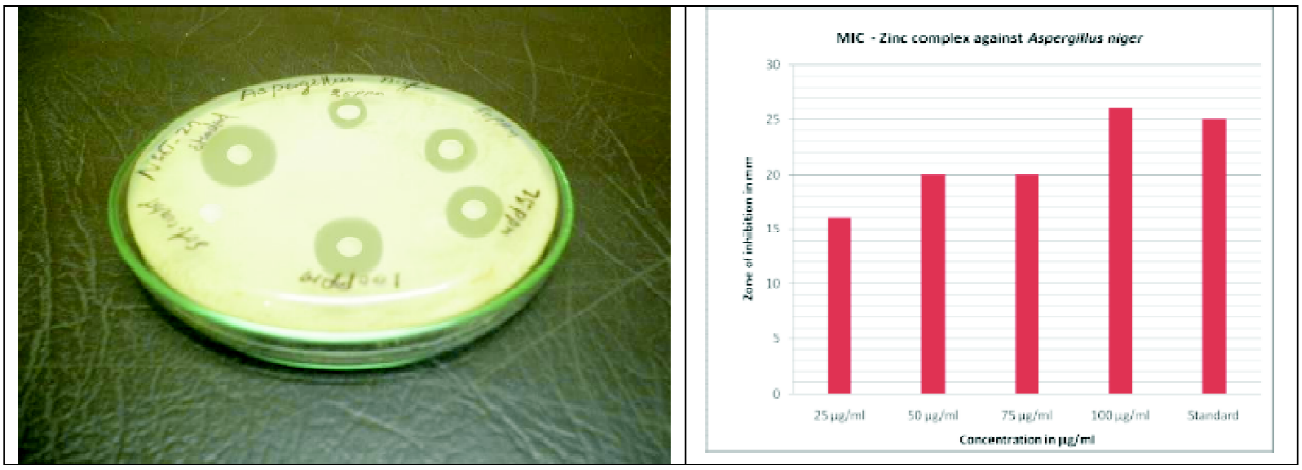

Fig. 4d. MIC of complex $[Zn(L)_2(H_2O)_2]$ against *Aspergillus niger.*

Table 3a. Antimicrobial property of HL and its metal(II) complexes

Sr. No.	HL/Metal complexes	Region of inhibition in mm					
		Bacteria (Gram-positive)		Bacteria (Gram-negative)		Fungi	
		Staphylococcus aureus (NCIM2079)	*Bacillus subtilis* (NCIM 2063)	*E. coli* (NCIM 2065)	*Klebsiella* sp. (NCIM 2098)	*Aspergillus niger* (NCIM 105)	*Candida albicans* (NCIM 3102)
	HL	13	10	10	12	10	12
1.	$[Mn(L)_2(H_2O)_2]$	10	14	10	16	15	22
2.	$[Co(L)_2(H_2O)_2]$	15	14	13	16	10	17
3.	$[Ni(L)_2(H_2O)_2]$	14	20	15	10	22	13
4.	$[Cu(L)_2(H_2O)_2]$	18	18	18	14	17	18
5.	$[Zn(L)_2(H_2O)_2]$	15	21	15	21	17	26

Table 3b. Minimum inhibitory concentration of highly active zinc complex

Metal complexes	Name of the microorganism	Region of inhibition in mm				Standard 100 µg/ml
		25 µg/ml	50 µg/ml	75 µg/ml	100 µg/ml	
$[Zn(L)_2(H_2O)_2]$	*Aspergillus niger*	16	20	20	26	25

Standard – Ciprofloxacin 5 µg/disc; Nystatin 100 units/disc for fungi
Solvent – DMSO.

concentration of 100 µg/ml. On diluting the concentration to 75 µg/ml the zone of inhibition values also decreases. The maximum value (20 mm) is observed for the complex. Further dilution to 50 and 25 µg/ml gradually decreases the biological effect against the fungal pathogens.

A relative study of zones of inhibition values explicitly shows, the metal complexes are effective inhibitors than the ligand. The data confirms the fact that the activity enhances significantly after complexation. Thus it is concluded that the metal complexes are excellent antimicrobial agents when compared to the parent ligand under identical conditions.

Antioxidant activity:

Antioxidant activity is a requirement for accomplishing many biological activities including anticancer, antiallergic, anti-inflammatory and anti-diabetic studies. The antioxidant activity of all the synthesized compounds with IC_{50} values is presented in Table 4. At the different concentrations of 5, 10, 50, 100 and 200 µg, ligand and complexes exhibit a much

Table 4. Antioxidant property of HL and its complexes

Sr. No.	Complexes	ABTS assay IC_{50} value (μM)	DPPH assay IC_{50} value (μM)
Ligand	HL	21.81	1437.63
1.	$[Mn(L)_2(H_2O)_2]$	45.61	1960.05
2.	$[Co(L)_2(H_2O)_2]$	120.62	3031.58
3.	$[Ni(L)_2(H_2O)_2]$	1988.27	3581.06
4.	$[Cu(L)_2(H_2O)_2]$	1618.23	3557.92
5.	$[Zn(L)_2(H_2O)_2]$	53.38	1959.74
Standard	Ascorbic acid	9.79	13.58

stronger ABTS scavenging property (Fig. 5a, 5b) relative to free ascorbic acid. If the IC_{50} value is low, the compound is found to be highly active. The antioxidant activity measured by DPPH radical assay does not show any prominent activity on comparing with standard ascorbic acid. The antioxidant activity of ligand measured by ABTS assay, shows very minimum IC_{50} value for the ligand HL and is nearer to the standard. A special monitoring of the complexes may give an idea about the antioxidant behaviour of the same ligand after complexation with different metal ions in ABTS assay. The comparison of IC_{50} values of all the compounds shows the following order: HL < $[Mn(L)_2(H_2O)_2]$ < $[Zn(L)_2(H_2O)_2]$ < $[Co(L)_2(H_2O)_2]$ < $[Cu(L)_2(H_2O)_2]$ < $[Ni(L)_2(H_2O)_2]$. Analysis of the complexes by the ABTS assay has remarkable antioxidant activity. More likely, manganese complex react with superoxide resulting in noticeable action in the indirect assays. The ligand has significant antioxidant activity, which is in close proximity to standard. After complexation with metal ions the activity slightly decreases, but the IC_{50} value is found to be minimum and less than 100 in ABTS assay.

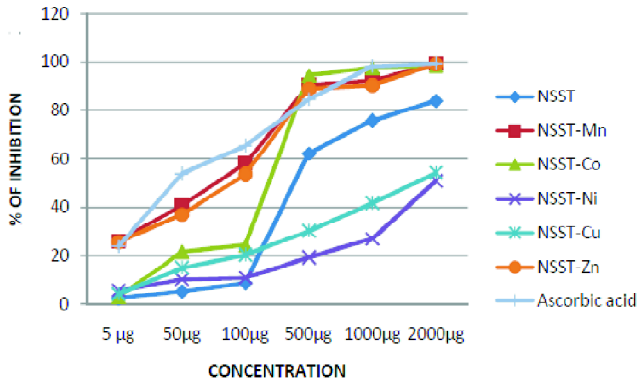

Fig. 5a. Antioxidant property of HL and its complexes(ABTS assay).

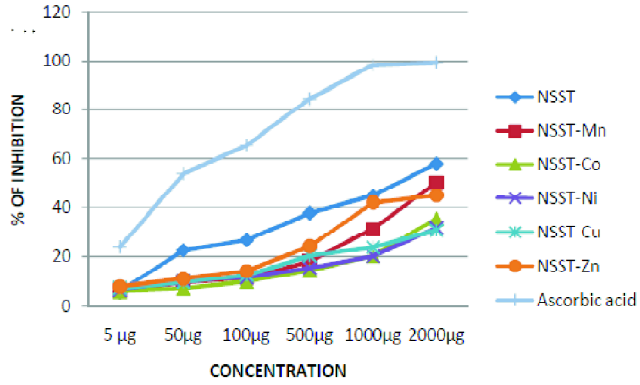

Fig. 5b. Antioxidant property of HL and its complexes (DPPH assay).

Conclusions

Bivalent mononuclear complexes of transition metal ions have been synthesized from new sulfonamide Schiff base obtained from sulfathiazole and 5-nitro salicylaldehyde. The structure of the synthesized complexes has been elucidated by physicochemical and analytical data. Mass spectral data are in consistency with the microanalytical data, confirming the composition and purities of the complexes (**1**-**5**). All the reported complexes are neutral and are having distorted octahedral geometry. Tentative structures have been proposed for the complexes which are shown below.

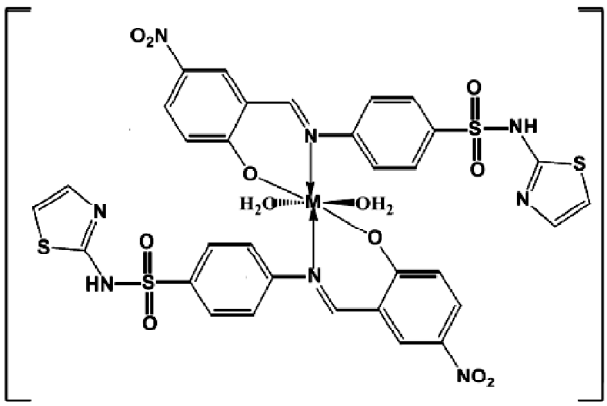

Where M = Mn(II), Co(II), Ni(II), Cu(II) and Zn(II)

The XRD pattern of complex **4** pronounces the crystalline character of the complex and the cell refinement parameters are also arrived at. It occupies face centered orthorhombic crystal system with the z value of 8. The redox

behaviour of the complexes has been determined by the cyclic voltammetric studies. A remarkable antioxidant activity has been observed for the reported ligand and it decreases on chelation with metals. On the reverse, the antimicrobial nature of the ligand has been increased on complexation with metal ions, due to increase in the lipophilic character of the metal.

Acknowledgements

The authors acknowledge Sophisticated Analytical Instrumentation Facility, Indian Institute of Technology, Chennai, Sophisticated Test and Instrumentation Centre, Cochin, Kerala, Central Electrochemical Research Institute,Karaikudi and SRM University, Kattankulathur for providing analytical support. In addition the authors are indebted to the Secretary, Principal and Faculty members of Chemistry, Seethalakshmi Ramaswami College, Trichy, Tamil Nadu for furnishing laboratory amenities and support.

References

1. F. Blasco, L. Perello, J. Latorre, J. Borras and S. Garcia-Granda, *J. Inorg. Biochem.,* 1996, **61**, 143.
2. L. S. Kumar, K. S. Prasad and H. D. Revanasiddappa, *Eur. J. Chem*., 2011, **2**, 394.
3. N. Sahu, S. Mondal, K. Naskar, S. Gupta, D. Kaleeswaran and C. Sinha, *J. Indian Chem. Soc.*, 2017, **94**, 1387.
4. D. Das, N. Sahu, S. Roy, P. Dutta, S. Mondal, E. L. Torres and C. Sinha, *Spectrochimica Acta A*, 2015, **150**, 268.
5. N. Sahu, D. Das, S. Mondal, S. Roy, P. Dutta, N. Sepay, S. Gupta, E. L. Torres and C. Sinha, *New J. Chem*., 2016, **40**, 5019.
6. N. Sahu, S. Mondal, N. Sepay, S. Gupta, E. T. Lopez, S. Tanaka, T. Akitsu and C. Sinha, *J. Biol. Inorg. Chem.*, 2017, **22**, 833.
7. S. Mondal, S. M. Mandal, T. Kumar Mondal and C. Sinha, *Spectrochimica Acta A*, 2015, **137**, 560.
8. M. S. Blois, *Nature*, 1958, **181**, 1199.
9. H. E. Muller, *J. Microbial. Methods,* 1984, **2**, 101.
10. J. F. Adediji, E. T. Olayinka, M. A. Adebayo and O. Babatunde, *Int. J. Phys. Sci.,* 2009, **4**, 529.
11. H. P. Ebrahimi, Z. A. Abdulnabi and Z. Boandnazar, *Spectrochim. Acta A,* 2014, **117**, 485.
12. M. Sonmez, *Turk. J. Chem.,* 2001, **25**, 181.
13. Gehad G. Mohamed, M. A. Zayed and S. M. Abdallah, *J. Mol. Struct.,* 2010, **979**, 62.
14. K. Ramakrishna Reddy and K. N. Mahendra, *Russ. J. Inorg. Chem.*, 2008, **53**, 906.
15. K. Nakamuto, in: "Infrared and Raman spectra of inorganic and coordination compounds", 5th ed., Hall Inc. Engle wood Chiffs, New Jersey, 1978.
16. I. Rama and R. Selvameena, *J. Chem. Sci.,* **127**, 671.
17. I. Rama and R. Selvameena *J. Indian Chem. Soc.,* 2014, **91**, 1877.
18. K. Singh, M. S. Barwa and P. Tyagi, *Eur. J. Med. Chem.,* 2006, **41**, 147.
19. Z. Hayvali, H. Unver and I. Svoboda, *Acta Chim. Solv.,* 2010, **57**, 643.
20. H. Zahid Chohan, T. Claudiu Supuran, *J. Enz. Inhib. Med. Chem.,* 2008, **23**, 240.
21. D. J. Pasto, in: "Organic structure determination", Prentice Hall International, London, 1969.
22. A. B. P. Lever, in: "Inorganic electronic spectroscopy", Elsevier, Amsterdam, New York, 1968.
23. D. N. Sathyanarayana, in: "Electronic absorption spectroscopy and related techniques", Universities Press (India) Limited, Hyderabad, 2001.
24. A. S. El-Tabi, M. E. Shakdofa and A. M. A. El-Seidy, *J. Korean Chem. Soc.*, 2011, **55**, 919.
25. M. Yongxiang, Z. Zhengzhi, M. Yun and Z. Gang, *Inorg. Chim. Acta,* 1989, **165**, 185.
26. P. W. Selwood, in: "Magneto chemistry", Interscience Publisher, London, 1956.
27. C. J. Balhausen, in: "Introduction to ligand field theory", Mc Graw Hill, New York, 1962.
28. B. N. Figgis, in: "Introduction to ligand fields", J. Wiley, New York, 1966.
29. R. L. Carlin, in: "Transition metal chemistry", Vol. I, Marcel Decker, New York, 1968.
30. A. P. B. Lever and J. Lewis, *J. Chem. Soc. A,* 1963, 2552.
31. N. Raman, S. Ravichandran and C. Thangaraja, *J. Chem. Sci.,* 2004, **116**, 215.
32. D. Kevelson and R. J. Niedman, *Chem. Phys.*, 1961, **35**, 149.
33. L. Saghatforoush, K. Adil, E. Sahin, S. Babaei and S. J. Muswvi, *J. Coord. Chem.*, 2011, **66**, 1463.
34. R. C. Maurya, D. Sutradhar, M. H. Martin, S. Roy, J. Chourasia, A. K. Sharma and P. Vishwakarma, *Arabian J. Chem.,* 2011, **8**, 78.
35. R. Jain, S. Karaiya, R. L. Yadav and V. K. Arya, *J. Sci. Ind. Res.,* 2012, **71**, 606.